OPTIMIZATION OF HYBRID RENEWABLE ENERGY SYSTEMS FOR A PUBLIC HOSPITAL: A CASE STUDY OF GRID AND OFF-GRID SOLUTIONS IN YALOVA, TURKEY

Asst. Prof. Dr. Aykut Fatih Güven
Yalova University, Faculty of Engineering,
https://orcid.org/0000-0002-1071-9700
Energy Systems Engineer Necat Uzuner
Yalova University, Faculty of Engineering,
https://orcid.org/0009-0005-0815-2580
Yusuf KAYA
Yalova University, Faculty of Engineering,
https://orcid.org/0009-0004-1949-7501
Sümeyra İBİŞ
Yalova University, Faculty of Engineering,
https://orcid.org/0009-0001-3268-5863

ABSTRACT

The growing global demand for energy and the depletion of fossil fuel resources have heightened the importance of renewable energy sources. Fossil fuel combustion not only degrades the environment but also contributes to climate change. This study presents a techno-economic feasibility analysis of hybrid energy systems for Yalova State Hospital, aiming to identify the most efficient configurations in both grid-connected and off-grid scenarios. The hybrid systems, consisting of photovoltaic (PV) solar panels, wind turbines, generators, and battery storage, were simulated and optimized in four distinct scenarios using HOMER software. Additionally, electric vehicle (EV) charging stations were integrated into all scenarios for further evaluation.

The results indicate that the most cost-effective grid-connected system is a PV panel, grid, and battery hybrid, with a net present cost of $15.5 million and a unit energy cost of $0.173/kWh. In the off-grid scenario, the optimal system consists of PV panels, a natural gas generator, and battery storage, with a net present cost of $26.2 million and a unit energy cost of $0.327/kWh. By improving energy independence and reducing carbon emissions, this study contributes to both environmental sustainability and the economic viability of transitioning to renewable energy sources.

Keywords: Hybrid Energy Systems, Techno-Economic Feasibility, Energy Optimization, Electric Vehicle Charging Stations

1. INTRODUCTION

The rapid increase in global population and industrialization has significantly elevated the demand for energy, creating a strain on the balance between energy production and consumption (Güven & Yörükeren, 2024). Energy plays a critical role across various sectors, including industry, transportation, and residential, making the transition to sustainable energy sources increasingly necessary. While fossil fuels have historically been the most widely used energy source, their limited and nonrenewable nature, along with their adverse environmental impacts, have raised concerns (Güven et al., 2023). The combustion of fossil fuels not only releases harmful greenhouse gases, contributing to climate change, air pollution, and ecosystem degradation, and leads to economic instability due to volatile fuel prices.

These challenges have prompted countries worldwide to rethink energy strategies and shift toward alternative energy sources (Al-Sahlawi et al., 2024).

Renewable energy sources, such as solar, wind, biomass, and geothermal energy, have emerged as vital solutions for sustainable energy production. These resources are not only environmentally friendly but also inexhaustible (Hasanien et al., 2024). By adopting renewable energy, countries can reduce their carbon emissions and enhance their energy independence. Countries like Germany have made significant strides in reducing their dependence on fossil fuels by utilizing high renewable energy sources. In 2022, Germany generated approximately 48.3% of its energy consumption from renewable sources, with onshore wind and photovoltaic systems contributing a significant portion. In the same year, Germany's onshore wind power production reached 100.5 TWh, representing a 12.4% increase from the previous year, while solar energy accounted for 11.4% of total electricity generation and biomass contributed 8.2% (Belkhier et al., 2024).

Turkey, similarly, has been actively transitioning toward renewable energy. According to the Turkish National Energy Plan, the country's electricity consumption is expected to reach 380.2 TWh by 2025 and 510.5 TWh by 2035. In 2022, Turkey generated 34.6% of its electricity from coal, 22.9% from natural gas, 20.3% from hydropower, 10.6% from wind, 5.1% from solar, and 3.4% from geothermal sources. These trends highlight the growing role for renewable energy investments in Turkey's energy landscape. As of November 2023, the country's installed capacity was 106,152 MW. As shown in Figure 1, Turkey's energy infrastructure by the end of 2023 includes a total installed capacity of 106,634.89 MW, an energy transmission line length of 74,034 km, and a total electricity production of 298.5 TWh, highlighting the country's significant advancements in energy production and transmission. Hybrid energy systems, which combine solar and wind energy, are designed to overcome the intermittency challenges of these individual sources and optimize energy supply (Güven & Yücel, 2023). Supported by energy storage systems, these hybrid configurations ensure a continuous supply of energy, even during insufficient sunlight or wind. Furthermore, the integration of natural gas generators into hybrid systems enhances reliability and reduces costs by preventing overcapacity (Chowdhury et al., 2023).

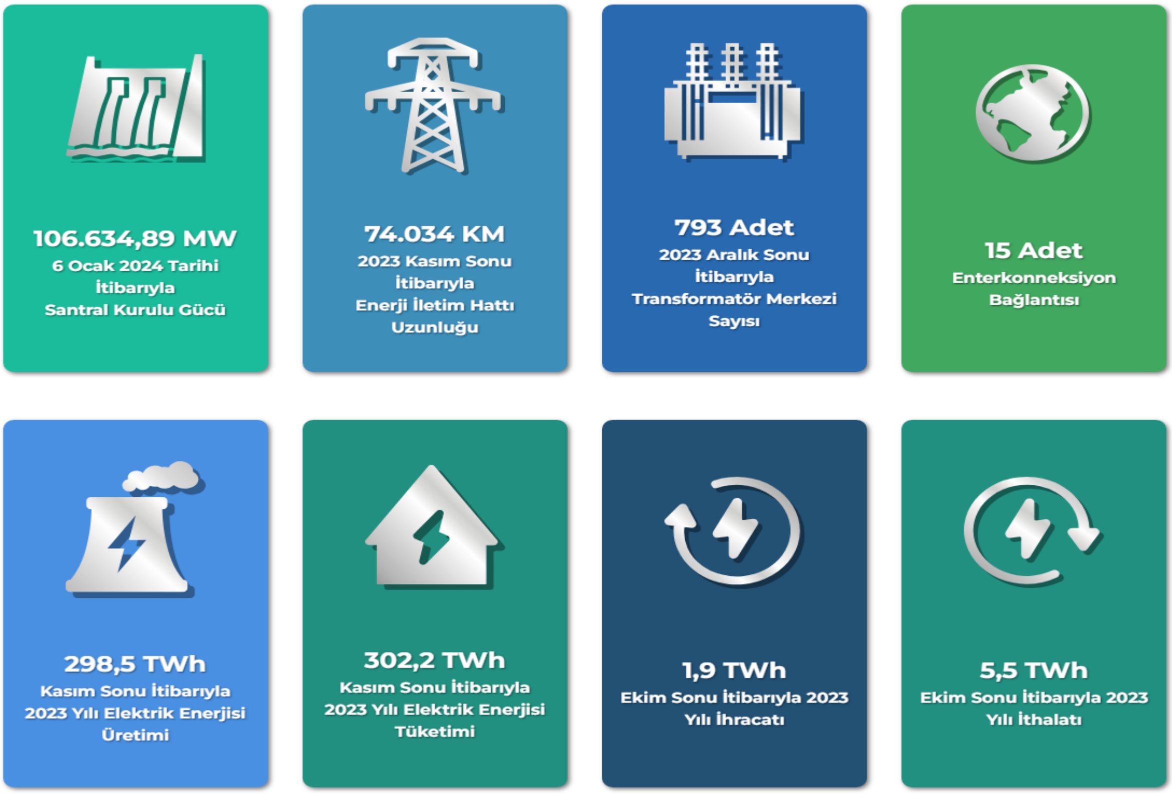

Figure 1. Turkey's energy status as of 2023.

This study examines the energy consumption data of the newly established Yalova State Hospital for the year 2023, aiming to evaluate both grid-connected and off-grid hybrid energy systems to meet the hospital's energy needs. The study simulates and analyzes four different system configurations, incorporating solar panels, wind turbines, generators, batteries, and electric vehicle charging stations, using HOMER software. The results focus on optimizing both cost efficiency and environmental sustainability.

2. METEOROLOGICAL DATA and LOAD PROFILES

2.1 Study Area

The study area is the newly constructed Yalova State Hospital, which is located 5.5 km from the city center of Yalova, in Turkey's Marmara Region (40° 63' 28" N, 29° 26' 62" E). The hospital occupies a 200-acre area with 105,000 square meters of indoor space and a parking capacity of 800 vehicles.

Figure 2. Yalova state hospital.

2.2 Solar Energy Potential

Consumption values for the selected load (Yalova State Hospital) were obtained from an analysis report conducted by Yalova University's Faculty of Engineering at the end of 2023. The amount of energy generated by installing solar panels to produce electricity is directly related to the region's meteorological data. The solar energy data for the region were obtained from the Yalova Meteorological General Directorate database. As illustrated in Figure 2, the solar energy potential of the region is higher during summer and lower during winter. Throughout the year, the average daily solar energy potential for the area has been measured at 4,205.01 kWh/m²/day.

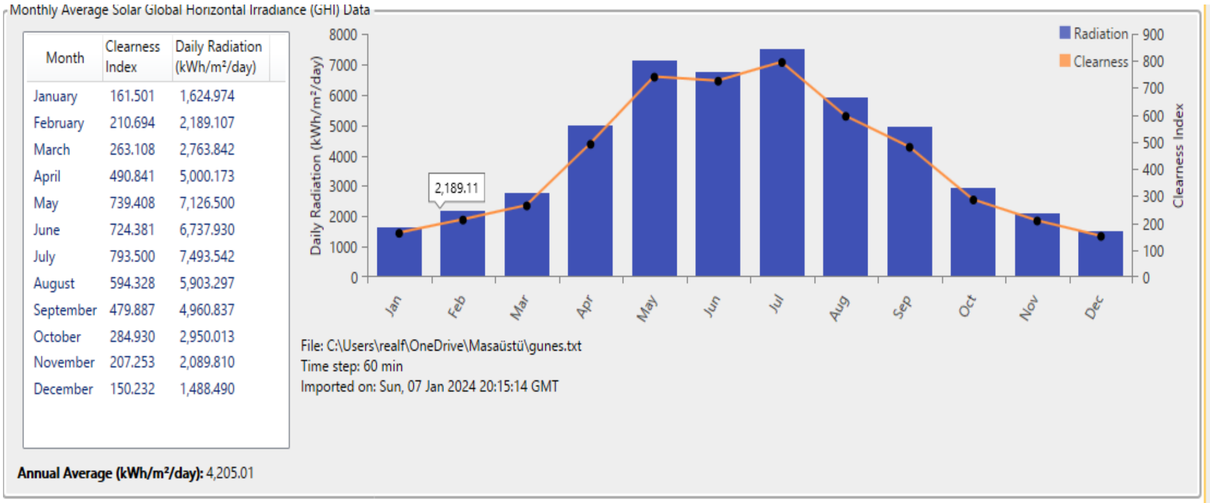

Figure 3. Monthly average solar radiation (kWh/m²/day) profile data of the region.

2.3 Wind Speed

The wind speed profile of a region is crucial because of the high investment costs of wind turbines. Prior to installation, it is essential to assess the wind speed profile at the potential site (Guven, 2024). Similar to solar energy potential, the wind speed data for the region were obtained from the Yalova Meteorological General Directorate's database, and the average wind speed was 1.99 m/s. Wind energy is considered a complementary source of energy, especially during winter when solar energy may be insufficient. Therefore, wind and solar energy are the two most common energy sources in hybrid systems. The wind speed profile of the region is shown in Figure 4.

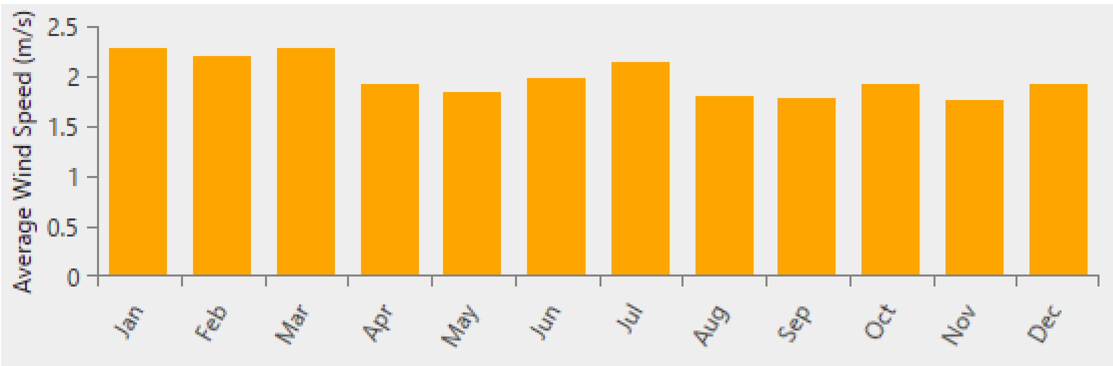

Figure 4. Monthly average wind speed (m/s) profiles of the region.

2.4 Temperature

The annual temperature data for the region are shown in Figure 5. Based on the data, temperatures increased between April and October. High temperatures can negatively affect the efficiency of solar panels. As the temperature rises, the electrical resistance within the panel increases, leading to a reduction in the amount of electricity generated. In general, a 1°C increase in temperature can result in approximately 0.5% decrease in panel efficiency. Additionally, temperature differences can create pressure variations that affect wind speed. Higher temperatures can increase air flow, potentially accelerating wind speed.

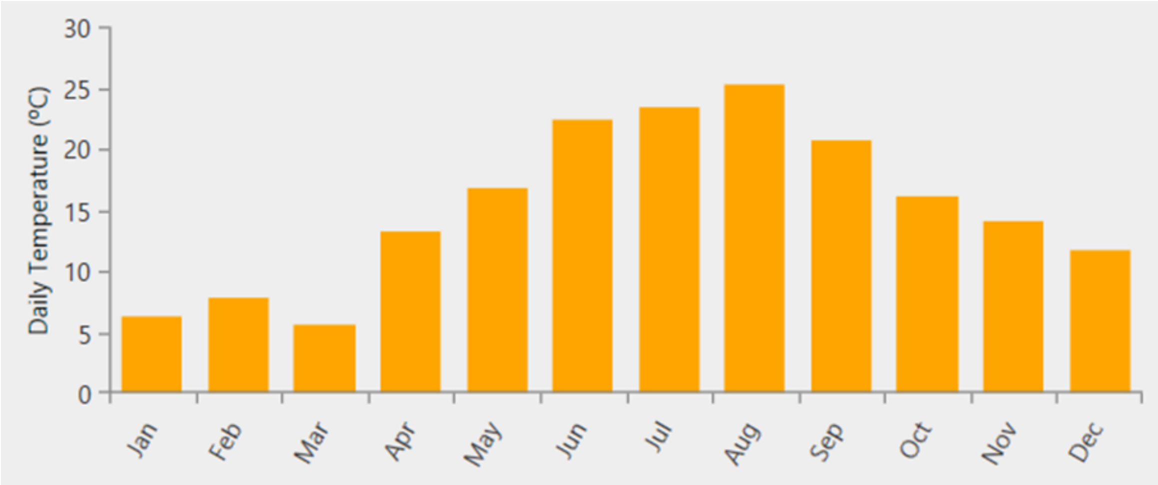

Figure 5. Annual temperature data of the region.

2.5 Electrical Load Profile

For the optimization process, the load profile of Yalova State Hospital was input into HOMER software to simulate and analyze various hybrid energy system scenarios. Understanding the hospital's electrical load profile is crucial in designing an efficient and reliable energy system because it directly affects the size of components such as solar panels, wind turbines, generators, and battery storage systems. By accurately mapping the load variations, the hybrid system can be designed to meet the hospital's energy demands, even during peak consumption periods.

Figure 6 (a) presents the annual load profile in heat map format, illustrating the hospital's energy demand throughout the year at different hours of the day. The horizontal axis represents the day of the year, and the vertical axis shows the hours of the day. The color spectrum ranging from blue to red indicates varying energy demands, with red areas representing peak loads. As shown in the figure, the energy demand tends to be higher during the daytime hours, especially in the summer months, likely due to increased cooling loads and medical equipment usage. The night-time demand remains relatively low throughout the year, except for specific periods when hospital operations require increased energy.

Figure 6 (b) shows the daily load profile, providing a clearer visualization of the hourly energy consumption pattern on a typical day. The peak load occurred at around 10:00 AM, reaching approximately 974.26 kW, which is in line with the hospital's highest activity levels. This peak is likely caused by the operation of critical medical devices, air conditioning, and lighting. The minimum load is observed at midnight (00:00), dropping to around 421.39 kW, reflecting the reduced demand during non-operational hours.

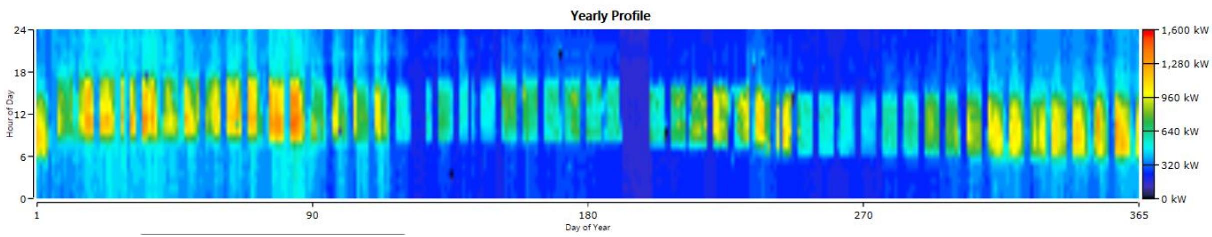

(a)

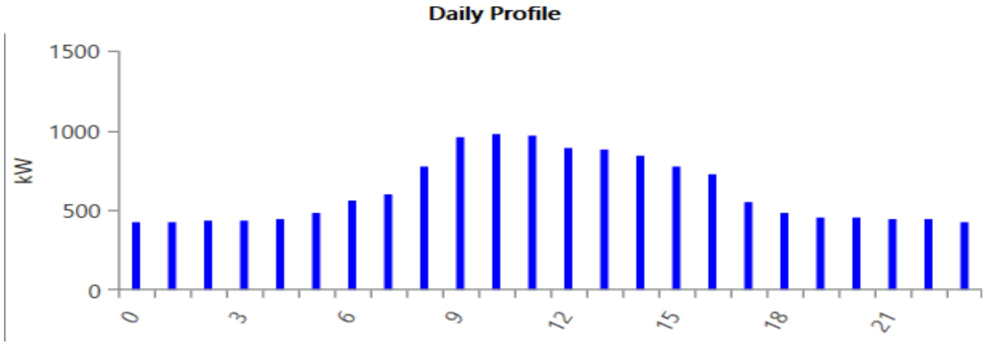

(b)

Figure 6. (a) Annual and (b) Daily electrical load profiles.

3. SYSTEM CONFIGURATION and COMPONENTS

3.1 Photovoltaic Panels

Photovoltaic (PV) panels consist of solar cells that convert sunlight into electrical energy. Solar energy is a renewable and environmentally friendly source of energy, making it a critical component of sustainable energy systems. In this study, SunPower E20-327 photovoltaic panels were selected as the solar energy system. These panels, with an efficiency rate of 20.4%, were simulated using HOMER software. The initial cost of the panels was estimated to be $400 per unit, with an annual maintenance cost of $50 and a lifespan of 25 years.

3.2 Wind turbines

Wind energy is a widely recognized renewable energy source valued for its environmental benefits, sustainability, and contribution to energy security. Wind turbines convert kinetic energy from the wind into electrical energy, which can be used for a variety of applications, including the industrial and transportation sectors. In the HOMER simulations, the selected wind turbine model was the generic 1 kW turbine with a hub height of 20 m. The turbine has an installation cost of $7,000, annual maintenance cost of $70, and a lifespan of 20 years.

3.3 Biodiesel Generator

Biodiesel is a biologically produced fuel derived from organic sources such as vegetable oils and animal fats. As a renewable alternative to conventional fossil fuels, it has been increasingly adopted for its reduced environmental impact. The biodiesel generator used in the system has a fuel cost of $1.609 per liter and an initial setup cost of $500. Additionally, the annual maintenance cost was $262.98, and the generator had a replacement cost of $500, and its lifespan was in line with these values.

3.4 Biomass Energy

Biomass energy is derived from organic materials such as plant and animal waste, wood, agricultural residue, and other biodegradable resources. Biomass can be used for electricity generation through direct combustion or converted into biogas via anaerobic digestion. Biogas, which primarily consists of methane, is produced by the fermentation of organic waste and can be used as an energy source for power generation. Biomass energy systems provide an effective means of utilizing waste materials for renewable energy production.

3.5 Battery Storage

Batteries play a crucial role in hybrid energy systems by storing energy and ensuring a stable power supply. They convert chemical energy into electrical energy and allow for energy storage during periods of excess production, which can later be used when the demand exceeds the supply. In this study, generic 1-kW li-ion batteries were selected with a minimum state of charge of 20% and an initial state of charge of 100%. Each battery has an energy storage capacity of 3,000 kWh, a voltage of 6 V, and a lifespan of 15 years. The annual maintenance cost of the battery system is $10.

3.6 Converters

Converters are critical components in hybrid energy systems and are responsible for converting alternating current (AC) to direct current (DC), and vice versa. AC converters are typically used to convert AC power from sources like the grid into DC for use in systems with batteries or other DC components. In contrast, DC converters adjust the DC voltage levels for distribution and control. The converter modeled in HOMER for this system has a cost of $300, zero annual maintenance cost, an efficiency rate of 95%, and a lifespan of 15 years (Güven & Poyraz, 2021).

3.7 Electric Vehicle Charging Stations

Electric vehicle (EV) charging stations are essential for supplying power to electric cars by transferring electrical energy to the battery. In this study, the daily energy consumption of the EV charging stations was set at 150 kWh, with a total capacity of 300 kWh. The maximum power output of each station is 300 kW, and the minimum load ratio is set between 20%, 50%, and 80% depending on the charging needs. These stations are crucial for supporting the increasing number of EVs and aligning hybrid systems with modern transportation demands (Jui et al., 2024).

4. HYBRID RENEWABLE ENERGY SYSTEM MODELING

4.1. HOMER Pro

HOMER Pro is a Microgrid Analysis and Optimization Tool developed by HOMER Energy LLC, a wholly owned subsidiary of Cummins, Inc. This globally recognized software is designed to perform comprehensive techno-economic analyses for hybrid microgrid systems that incorporate various energy sources. HOMER Pro simulates the performance of different energy system configurations under varying conditions, evaluating them based on key performance indicators, such as total net present cost, levelized cost of energy, renewable energy fraction, and excess electricity. This detailed analysis provides users with critical insights into cost-effective and reliable system configurations (Diaf et al., 2008).

One of the key features of HOMER Pro is its compatibility with a broad range of power systems, including off-grid, on-grid, and battery-supported systems. The software allows users to compare the results of various design and technology options, thus aiding in understanding their impact on the overall system performance. Additionally, HOMER Pro can account for potential changes in future fuel and electricity prices, making it a powerful tool for resilience planning and energy system optimization.

With its user-friendly interface and robust capabilities, HOMER Pro has become the standard tool for analyzing and optimizing energy systems in the global renewable energy sector.

4.2 Off-Grid System Optimization

In the optimization process of the off-grid system, a single-line diagram was configured to integrate the natural gas generator, wind turbine, and load profile into the AC line. On the DC line, the components connected are the photovoltaic panels, battery storage systems, and EV charging stations. A bidirectional converter was used to link both the AC and DC lines to allow energy flow in both directions. Figure 7 shows the best scenario diagram for an off-grid system.

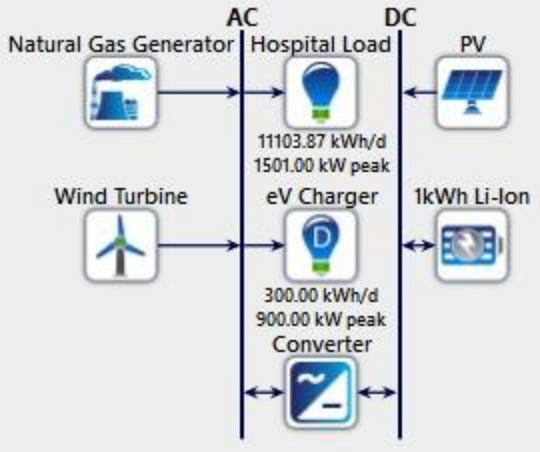

Figure 7. Off grid best scenario diagram.

Before optimization, the meteorological data, technical and economic parameters, and baseline load profile data (compiled for over 8,760 hours) of the system components were incorporated into the optimization process. The resulting configuration was then evaluated from technical, economic, and environmental perspectives to ensure the system's overall viability.

4.3 On-Grid System Optimization

For the on-grid system optimization, a similar single-line diagram was used, where the natural gas generator, wind turbine, grid connection, and load profile were integrated into the AC line. The photovoltaic panels, battery storage systems, and electric vehicle charging stations were connected to the DC line. As in the off-grid scenario, a bidirectional converter was employed, enabling efficient energy flow between the AC and DC components. Figure 8 shows the best scenario diagram for an on-grid system.

As in the off-grid scenario, meteorological data, technical and economic parameters, and the baseline load profile (also compiled for over 8,760 hours) were included in the optimization process (Güven & Mengi, 2023). The system configuration was evaluated across multiple dimensions, including technical performance, economic feasibility, and environmental impact.

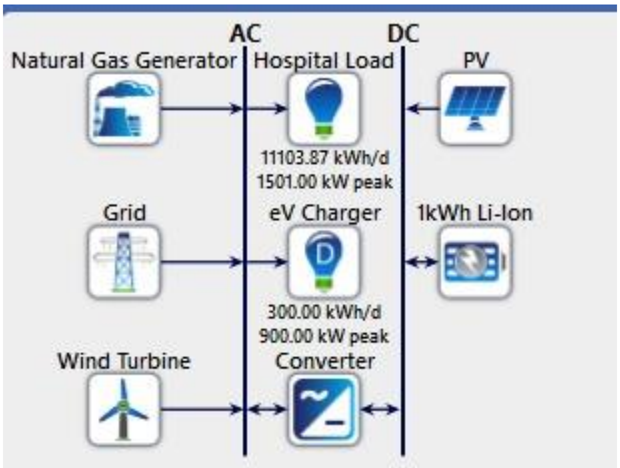

Figure 8. On-grid best scenario diagram.

5. HYBRİD RENEWABLE ENERGY SYSTEM COMPONENTS

5.1 Photovoltaic (PV) Panels

Photovoltaic (PV) systems generate clean energy when exposed to sunlight, converting solar radiation directly into electricity. In the HOMER Pro system, SunPower E20-327 PV panels with a capacity of 1 kW were selected. The cost parameters for the PV system are defined as follows: an initial capital cost (ICC) of $650, a replacement cost (RC) of $650, and an annual operation and maintenance (O&M) cost of $50. Based on these assumptions, simulations were conducted. The power output of the PV panels can be calculated using Equation (1) (Falope et al., 2024):

$$P_{PV} = Y_{PV} \times f_{PV} \times \left(\frac{G_T}{G_{T.STC}}\right) \times [1 + \alpha_f \times (T_C - T_{C.STC})] \qquad (1)$$

Where:

- P_{PV} (kW) is the power output of the PV system at any given time,
- Y_{PV} (kW) denotes the nominal output power under the standard test conditions (STC),
- f_{PV} is the PV degradation factor
- G_T (kW/m²) represents the solar irradiance at the time
- $G_{T.STC}$ (1 kW/m²) is the solar irradiance in the STC
- α_f (%/°C) is the temperature coefficient of the PV panel as follows:
- T_C is the PV module temperature, and
- $T_{C.STC}$ (°C) is the temperature at the STC (25°C).

If the temperature effect α_f is not considered in HOMER Pro, the PV power output is calculated using this equation.

5.2 Wind Turbine (WT)

Wind turbines convert kinetic energy from the wind into mechanical energy, which is subsequently transformed into electricity. For this system, a generic 1 kW wind turbine was chosen owing to its efficiency and suitability for energy systems. The economic parameters for the wind turbine are defined as follows: an ICC of $7,000, an RC of $7,000, and an annual O&M cost of $70. The turbine has a hub height of 20 m and an operational lifespan of 20 years (Güven & Yörükeren, 2022).

HOMER Pro software was used to calculate the power output of the wind turbine in three steps. First, the wind speed at the hub height was calculated using Equation (2) (Güven & Yücel, 2024):

$$U_{hub} = U_{anem} \times \frac{\ln(\frac{Z_{hub}}{Z_0})}{\ln(\frac{Z_{anem}}{Z_0})} \qquad (2)$$

Where:

- U_{hub} (m/s) is the wind speed at the hub height.
- U_{anem} (m/s) is the wind speed at the anemometer height.
- Z_{hub} (m) is the hub height.
- Z_{anem} (m) is the anemometer height.
- Z_0 (m) is the surface roughness length.

Based on this wind speed, the expected power output of the wind turbine was estimated using the turbine's power curve, as shown in Figure 9. Finally, HOMER Pro adjusts this power output by factoring in the air density using the following equation, thereby producing the actual output power facilitated by the wind turbine.

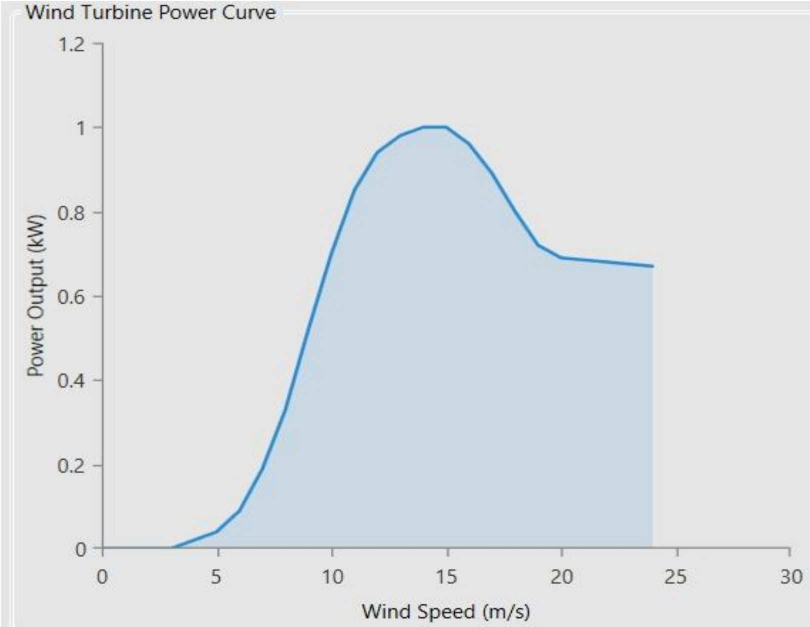

Figure 9. Wind turbine power curve.

$P_{WTG} = (\frac{\rho}{\rho_0}) \times P_{WTG,STC}$

(3)

Where:

- P_{WTG} is the actual power output of the wind turbine (WTG) under the current conditions.
- ρ (kg/m³) is the air density at the current location and altitude, respectively,
- ρ_0 (kg/m³) is the air density under standard temperature and pressure (STP) conditions, and
- $P_{WTG,STC}$ is the power output of the wind turbine under the standard test conditions (STC).

5.3 Generators

The thermal energy produced by fuel combustion is converted into mechanical energy, which is then used to generate electricity. Depending on the fuel type, generators can vary in terms of performance and efficiency. This study uses diesel, biodiesel, and biogas generators.

5.3.1 Diesel Generator (DG)

A diesel generator is used as a backup power source when the electricity produced by the PV array and stored in the battery bank is insufficient to meet the load demand. The fuel consumption of the DG is directly related to the amount of electricity generated. In this simulation, a fuel cost of $1 per liter was assumed. The economic parameters for the DG are: an ICC of $250, an RC of $250, and an annual O&M cost of $30. The fuel consumption rate, which depends on the generator's power output, was calculated using Equation (4) (Güven, & Mete, 2021):

$$F(t) = (F_0 \times Y_{gen}) + (F_1 \times P_{gen}) \quad (4)$$

Where:

- $F(t)$ represents the fuel consumption rate,
- F_0 (L/h/kW) is the fuel curve intercept coefficient,
- F_1 (L/h/kW) is the slope of the fuel curve.
- Y_{gen} (kW) is the rated power under the STC, and
- P_{gen} (kW) is the generator's output power at time t.

5.3.2 Biodiesel Generator

Biodiesel generators use renewable biodiesel fuel, typically derived from vegetable oils or animal fats, to generate electricity. These generators are a more environmentally friendly alternative to conventional diesel generators.

5.3.3 Biogas Generator

Biogas generators produce electricity using biogas, which is derived from the anaerobic fermentation of organic waste materials such as animal manure, plant residues, and food waste. Biogas, primarily composed of methane, is a renewable fuel source that offers a sustainable means of power generation.

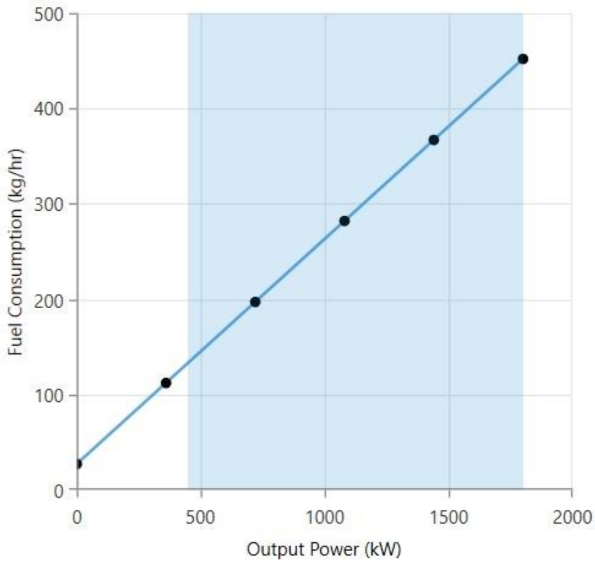

Figure 10. Biogas fuel power curve.

5.4 Battery Storage System

The batteries store excess electricity generated by renewable sources, allowing the system to maintain power supply during periods of low electricity generation. In this study, a generic 1-kWh Li-Ion battery was selected for the system. The economic parameters for the battery are as follows: an ICC of $550, an RC of $550, and an annual O&M cost of $10. The battery depth of discharge (DOD) was set to 80%. The number of batteries required for the system was calculated as follows (Güven, 2017).:

$$N_{bat} = \frac{E_d \times n_d}{V_{bat} \times Ah \times DD} \qquad (5)$$

Where:

- E_d (kWh) represents the daily energy demand.
- n_d is the number of days of autonomy.
- V_{bat} is the battery voltage.
- Ah (Ah) is the battery capacity, and
- DD is the discharge depth.

5.5 Grid Integration

In the HOMER Pro system, electricity pricing and sales rates are based on time-of-use tariffs. The T3 peak electricity tariff, as applied in Turkey, was integrated into the system. The tariff structure is as follows:

- Rate 1 (06:00–17:00): electricity price of $0.1600/kWh and sales price of $0.1000/kWh.
- Rate 2 (17:00–22:00): electricity price of $0.1800/kWh and sales price of $0.1000/kWh.
- Rate 3 (22:00–06:00): electricity price of $0.1200/kWh and sales price of $0.1000/kWh.

This pricing structure plays a critical role in optimizing energy costs by encouraging reduced consumption during peak hours.

5.6 Converter

A converter is an essential component that facilitates the conversion of alternating current (AC) to direct current (DC). In hybrid energy systems, a converter is required to manage the energy flow between AC and DC components, including PV panels, wind turbines, and battery storage. The converter used in this system has an efficiency of 95%. The economic parameters for the converter are: an ICC of $300, an RC of $300, and an annual O&M cost of $50. The converter capacity is calculated using Equation (6) (Güven, & Hatipoğlu, 2022).:

$$P_{inv} = \frac{E_{L,max}}{\eta_{DC/AC}} \quad (6)$$

- P_{inv} (W) is the inverter's capacity.
- $E_{L,max}$ (Wh) is the maximum energy demand of the load
- $\eta_{DC/AC}$ is the conversion efficiency.

6. SIMULATION RESULTS and DISCUSSION

This section presents the simulation outcomes, focusing on the sensitivity analyses and system performance under different conditions. The objective is to understand how key factors, such as photovoltaic panel derating and fuel price fluctuations, impact the system's overall efficiency, cost, and output. The following subsections detail the sensitivity analyses performed for the off-grid and on-grid scenarios.

6.1 Sensitivity Analysis

Sensitivity analysis plays a crucial role in evaluating how different parameters influence the performance and economic viability of hybrid energy systems. By varying factors such as photovoltaic panel deducting and natural gas fuel prices, we can assess the system's adaptability and long-term resilience.

6.1.1 Impact of Photovoltaic (PV) Panel Derating Factor on System Performance

The PV panel derating factor refers to the power output reduction relative to the nominal output under specific conditions. Factors such as temperature, shading, dirt, mismatch loss, and panel degradation contribute to this derating.

This factor is typically expressed as a percentage and is used in the design and analysis of solar PV systems to account for real-life performance. It allows designers and installation contractors to factor in potential losses and optimize the system performance. By adjusting the derating factor, the system can be ensured to meet the performance requirements under actual operational conditions.

In our analysis, we employed three different percentages to represent the PV derating factor, aiming to assess the impact of these factors on the overall system performance, output, and financial outcomes. By examining these effects, we gain insights into how system design and operation can be optimized to enhance performance and longevity.

Figure 11 (a) illustrates the impact of the derating factor on the PV capacity and energy cost in the optimal off-grid scenario. In the best on-grid scenarios, no such analysis was performed due to the absence of PV panels in the optimal on-grid configuration.

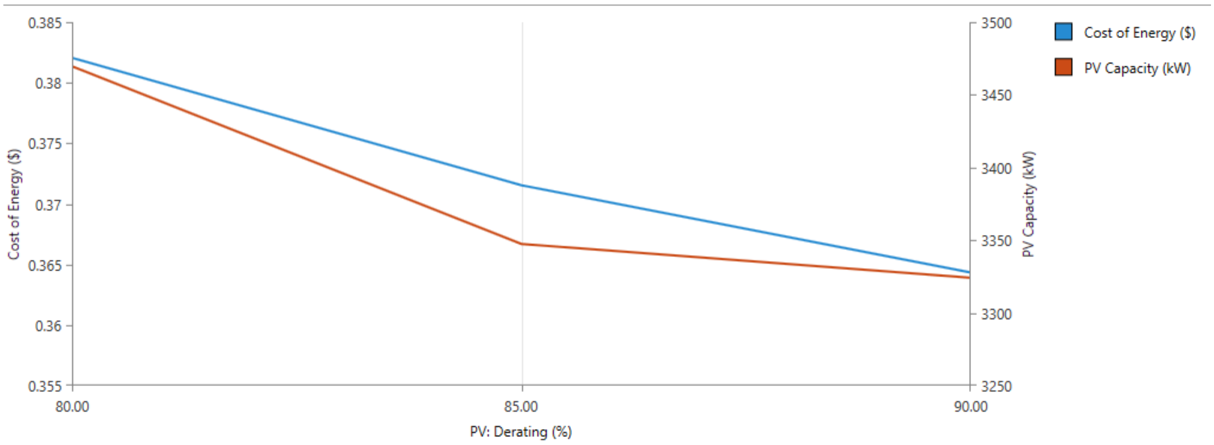

(a)

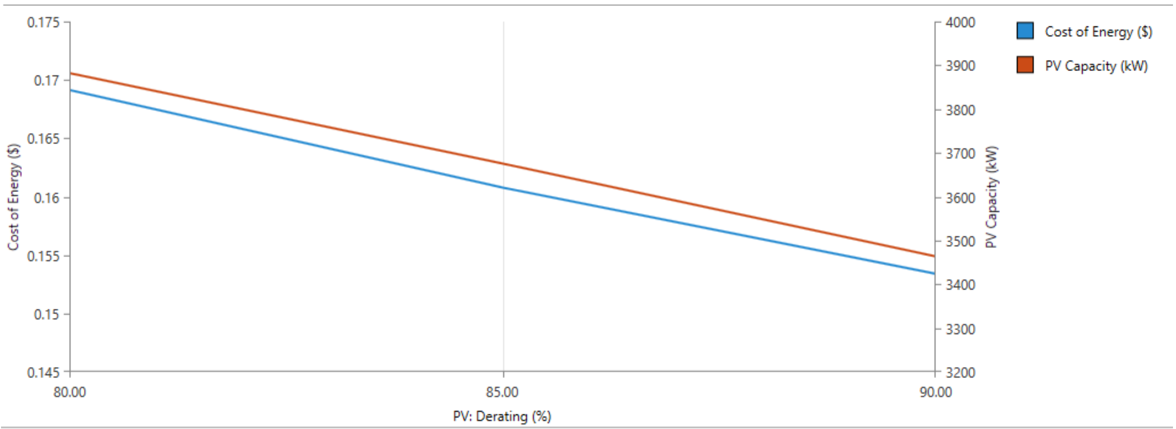

(b)

Figure 11. PV impact of the derating factor: (a) Off-grid and (b) On-grid.

As shown, an increase in the derating factor results in a decrease in energy costs (from $0.382 to $0.365) and a corresponding reduction in photovoltaic capacity. This trend highlights the trade-offs involved in adjusting the derating factors, emphasizing the balance between cost optimization and system performance in off-grid scenarios.

Similarly, for the on-grid scenario, the increase in the derating factor reduced energy costs (from $0.168 to $0.153) and photovoltaic capacity. This trend underscores the delicate balance between system efficiency and economic considerations in off-grid and on-grid PV installation. Although the derating factor reduces the photovoltaic capacity by decreasing efficiency, it simultaneously lowers the upfront investment required, resulting in reduced energy costs. This balance illustrates the trade-off between performance and financial optimization in off-grid and on-grid PV systems.

Considering the derating factors in a system design offers numerous advantages, including optimized performance, accurate cost analysis, enhanced reliability, improved system design, and financial optimization.

6.1.2 Impact of Varying Natural Gas Fuel Prices on System Performance

In the sensitivity analysis conducted within the simulation, we hypothesized that natural gas prices for the generator may increase over time, potentially reaching $0.17, $0.20, and $0.25 per unit. Similarly, biomass fuel prices could also increase, with projected prices reaching $38.00, $41.40, and $45.00 per ton. This approach allowed for a detailed investigation of the system's response to fuel cost fluctuations, providing deeper insights into the system's long-term feasibility and resilience against market volatility.

Figure 12(a) demonstrates the impact of changing natural gas prices on energy cost and generator output, while Figure 12(b) shows the impact of fluctuating biomass prices on the same parameters.

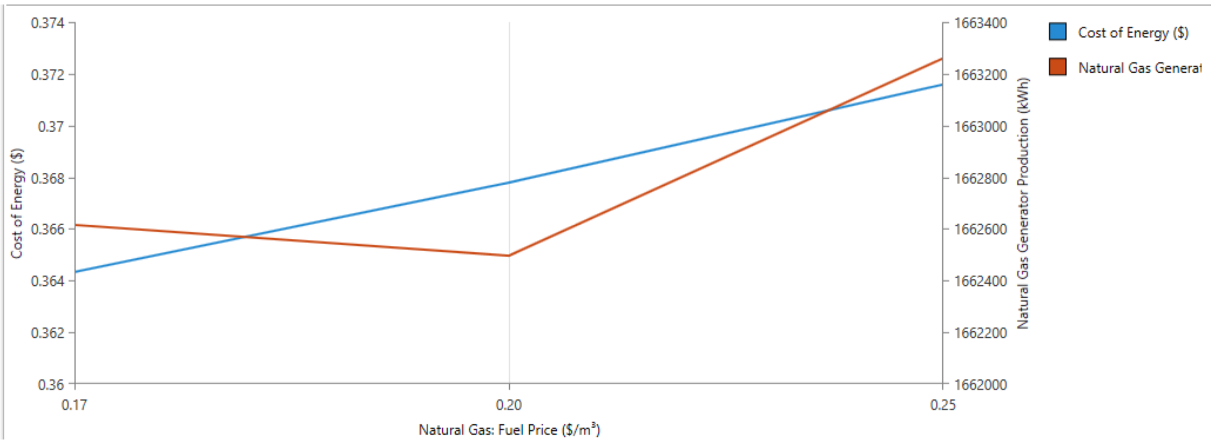

(a)

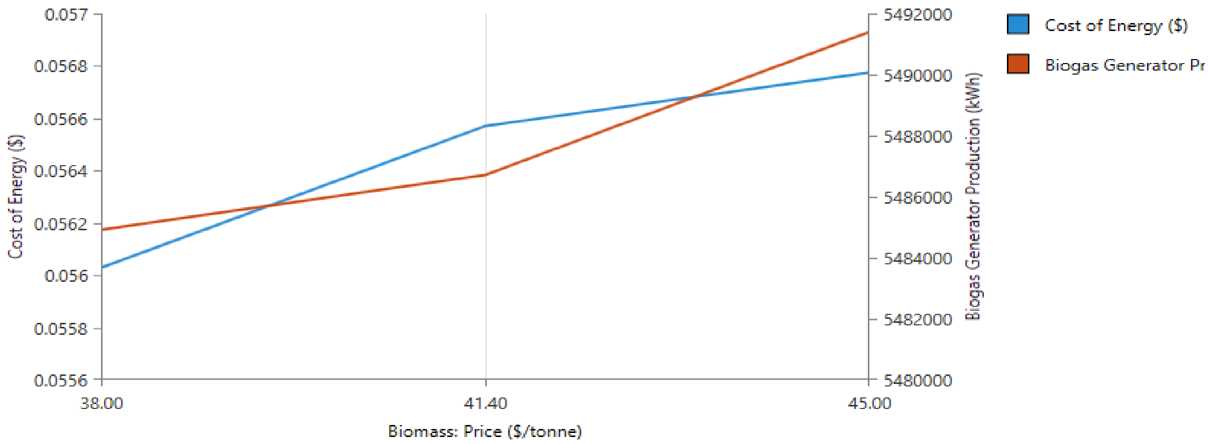

(b)

Figure 12. impact of varying fuel prices (a) Off-grid and (b) On-grid.

The increase in natural gas prices resulted in an increase in energy costs, from $0.364 to $0.372 per kWh. However, as fuel prices increased, kWh production from the natural gas generator initially decreased and then increased again, indicating that the system favored other components for cost-effective power generation as gas prices rose. This demonstrates that the system consistently adjusts to provide the most efficient and optimal results.

In the on-grid system, changes in natural gas prices had no impact on the energy cost or the generator's output. This is because, in the optimal on-grid scenario, the system relies primarily on the grid, battery, PV panels, and converter, with no need for a natural gas generator. Therefore, natural gas price fluctuations do not affect the on-grid system's performance.

In conclusion, analyzing changes in fuel prices provides valuable insights into system dynamics. As natural gas prices rise, there is a noticeable increase in energy costs and a temporary decrease in the generator's output. In contrast, changes in biomass prices lead to a proportional increase in both energy costs and biogas generation. These findings emphasize the system's adaptive response to fluctuating fuel prices and highlight the cost-effectiveness and operational efficiency. By strategically allocating resources and adjusting production mechanisms in response to market conditions, the system maintains its economic resilience while achieving the desired outcomes. [2]

6.1.3 Effect of Renewability Ratio on System Performance

Renewability ratios typically represent the proportion of energy derived from renewable sources to total energy consumption or production. This metric is frequently used to assess the share of renewable energy within a specific energy system or grid. Renewability fractions can be calculated over various time scales (e.g., annual, monthly, or hourly) and for different scopes (e.g., national, regional, or local). For instance, if a country generates 30% of its electricity from renewable sources such as solar, wind, hydro, and biomass, then the renewable fraction for electricity generation would be 30%. Similarly, if a community aims for a 50% renewable fraction of total energy consumption, then half of the consumed energy comes from renewable sources.

Understanding renewable fractions is critical for evaluating progress toward renewable energy targets, assessing the environmental impact of energy systems, and informing policy decisions aimed at promoting sustainable energy practices.

In this simulation, two renewable ratios—40% and 60%—were analyzed. Figure 13(a) illustrates the effect of the renewability ratio on energy cost and carbon dioxide emissions in the off-grid scenario, while Figure 13(b) demonstrates the same effect in the on-grid scenario.

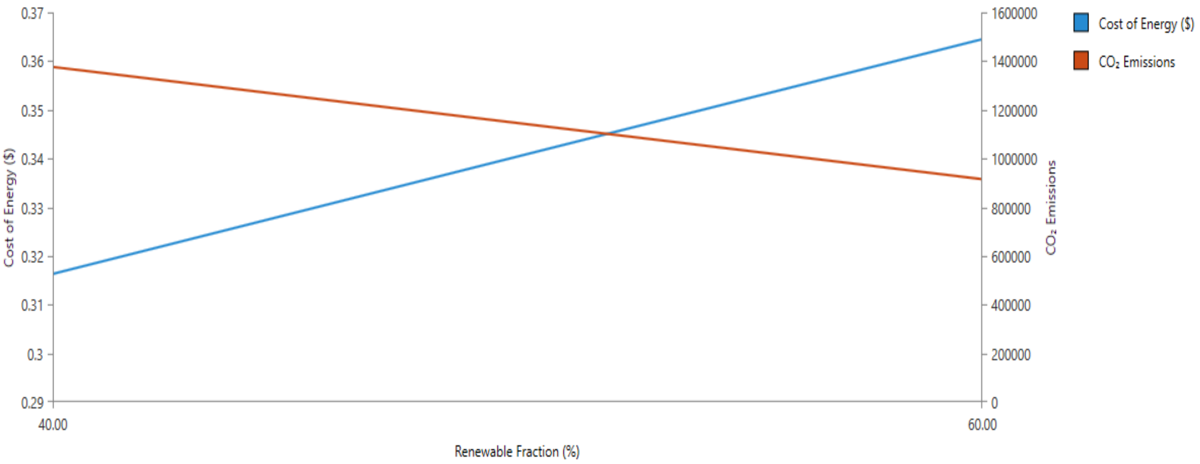

(a)

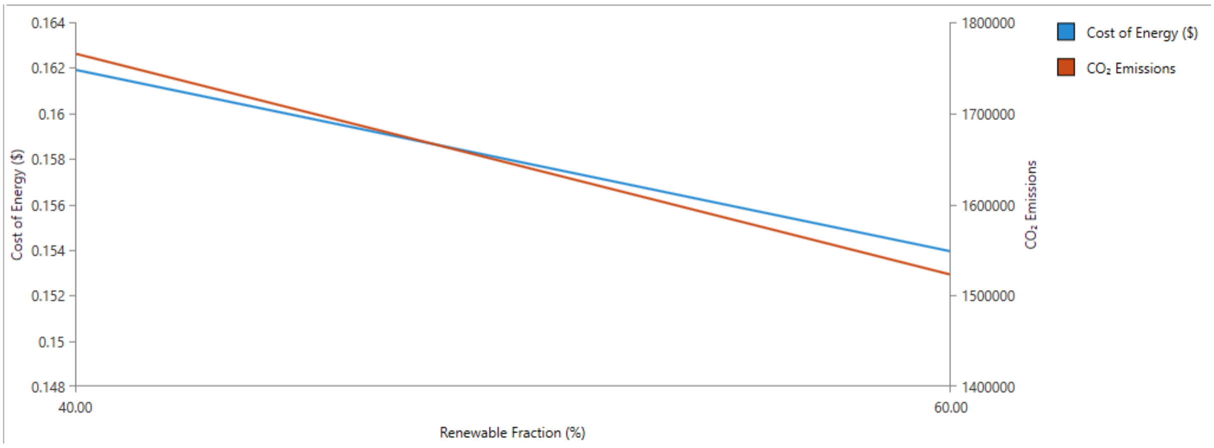

(b)

Figure 13. Effect of renewable fraction ratio (a) Off-grid and (b) On-Grid.

From Figure 13(a), it can be observed that increasing the renewability ratio leads to an increase in energy costs, from \$0.320 to \$0.365 per kWh. This is primarily due to the higher costs associated with renewable energy compared to fossil fuel sources. The simulation shows that while 40% renewable fraction reduces costs, it simultaneously increases carbon emissions. This is because the greater the share of renewable and clean energy used, the lower the carbon emissions and the lower the environmental impact.

In the future, as renewable energy technologies continue to develop and become more cost-effective, we expect a transition toward higher renewable fractions. This will lead to cleaner and more sustainable energy systems, which are likely to outperform fossil fuel-based systems in terms of both cost and efficiency.

In the on-grid scenario, as shown in Figure 13(b), increasing the renewability ratio reduces energy costs from $0.162 to $0.155 per kWh. This can be explained by the fact that as the renewability ratio increases, the cost of energy (COE) decreases but the net present cost rises. This is because drawing energy from the grid is more economically favorable than installing new renewable energy systems. While increasing the renewability ratio by adding more renewable resources raises the initial investment cost, the system continues to favor grid-based solutions because of their cost-effectiveness, as seen in the optimal scenario.

6.1.4 Effect of Wind Turbine Tower Height on System Performance

The height of wind turbine towers significantly affects the power output of the turbines. As the elevation increases, the wind speed tends to increase due to reduced surface roughness and fewer obstructions from land features. Consequently, taller towers allow wind turbines to access stronger and more consistent wind resources, resulting in higher power generation.

The relationship between wind speed and power output follows a cubic function called the power curve. Even small increases in wind speed can substantially improve power output. Taller towers also enable the installation of larger rotors, which allows turbines to capture more wind energy, further enhancing their efficiency.

In general, taller wind turbine towers play a critical role in maximizing the energy production potential of wind turbines by achieving higher wind speeds and enabling more efficient energy capture.

However, in this simulation, no significant analysis or graphics were presented regarding the effect of wind turbine height on system performance. This is because the region under study—Yalova—has very low annual average wind speeds, which directly affect the efficiency of wind turbines.

The HOMER Pro simulation indicated that adding a wind turbine to the system would have a negative impact on the overall system cost, making its use impractical. As a result, although wind turbines were included in the scenarios, they were not utilized in the optimal solutions due to their lack of economic feasibility in this specific region.

6.1.5 Impact of Average Daily Electricity Consumption of Electric Vehicle Charging Stations on the System

The average daily electricity consumption of EV charging stations is influenced by a variety of complex factors, all of which must be carefully analyzed to understand their effects on the system. One of the most critical factors determining consumption is the type of charging station. Fast-charging stations, which provide high-power electricity to charge vehicles more quickly, typically consume between 100 and 500 kWh per day. In contrast, slow-charging stations operate at lower power and consume between 10 and 50 kWh daily. The power capacity of the station plays a significant role in shaping its overall electricity demand.

Another crucial factor influencing daily electricity consumption is the frequency of usage. Stations located in high-traffic areas or frequently used by EV owners naturally consume more electricity because of the higher number of vehicles being charged. Conversely, stations with lower usage experience correspondingly lower consumption. The demand for charging at a particular station is often determined by its geographic location and the density of EV users in that region.

In addition, the battery capacity of the vehicles being charged plays an important role in determining the electricity consumption. Vehicles with larger batteries require more electricity to reach full charge, whereas those with smaller batteries consume less energy. For instance, when a vehicle with a large battery is charged, it significantly increases the daily consumption of the station, whereas smaller battery vehicles require less energy, thereby reducing the overall demand. Thus, the technical specifications of vehicles that use charging stations directly affect the total electricity consumption.

Regional electricity grid characteristics and pricing policies also have a notable impact on the total electricity consumption of EV charging stations. In regions where electricity prices are low, there is likely to be a greater demand for charging, as users are encouraged to take advantage of lower costs. Conversely, in areas with high electricity prices, users may reduce their charging frequency, leading to lower consumption. Seasonal factors also contribute to variations in electricity consumption. In colder months, for example, lower temperatures can increase the charging time because EVs may require more energy to maintain optimal battery performance, thus increasing the consumption. In warmer months, high temperatures may affect battery efficiency, which can either increase or decrease the consumption depending on specific conditions.

Given the interplay of these factors, the daily electricity consumption of EV charging stations can vary widely, ranging from 10 to 500 kWh. The simulation results further highlight these variations. As shown in Figure 7, the average daily electricity consumptions of charging stations under different sensitivity conditions is observed to be 220 kWh, 280 kWh, and 300 kWh, respectively. The corresponding energy costs for these consumption levels were calculated as $0.311, $0.316, and $0.310, respectively. These data illustrate that, in general, energy costs also increase as consumption increases. However, the slight reduction in cost observed at the 300-kWh consumption level suggests that higher consumption may lead to lower unit energy costs in certain scenarios. This can be attributed to bulk energy purchase discounts or time-based pricing models.

From an annual electricity production perspective, daily consumption levels also have a direct impact. With a daily consumption of 220 kWh, the annual electricity production is calculated to be 4.8 million kWh. Similarly, for daily consumption levels of 280 and 300 kWh, annual electricity production reaches 4.5 million and 4.86 million kWh, respectively. These results indicate that higher daily consumption typically leads to increased annual production, whereas lower consumption results in decreased production. Differences in annual electricity production are influenced by variations in daily consumption, system efficiency, energy sources, and environmental conditions.

Furthermore, the data presented in Figure 8 emphasize the correlation between daily consumption levels and energy costs. For a daily consumption of 220 kWh, the energy cost is calculated to be $0.1573, while for 280 kWh, the cost is $0.1539, and for 300 kWh, it is $0.15392. These findings suggest that even small changes in daily consumption can significantly affect both energy costs and annual electricity production.

In summary, the average daily electricity consumption of EV charging stations has a complex and multi-dimensional impact on energy costs and annual electricity production. By analyzing the system's efficiency, energy pricing models, and consumption patterns, it is possible to optimize the energy management of charging stations and achieve more efficient operation. The data presented in Figures 7 and 8 offer valuable insights into the effects of daily consumption on long-term system performance.

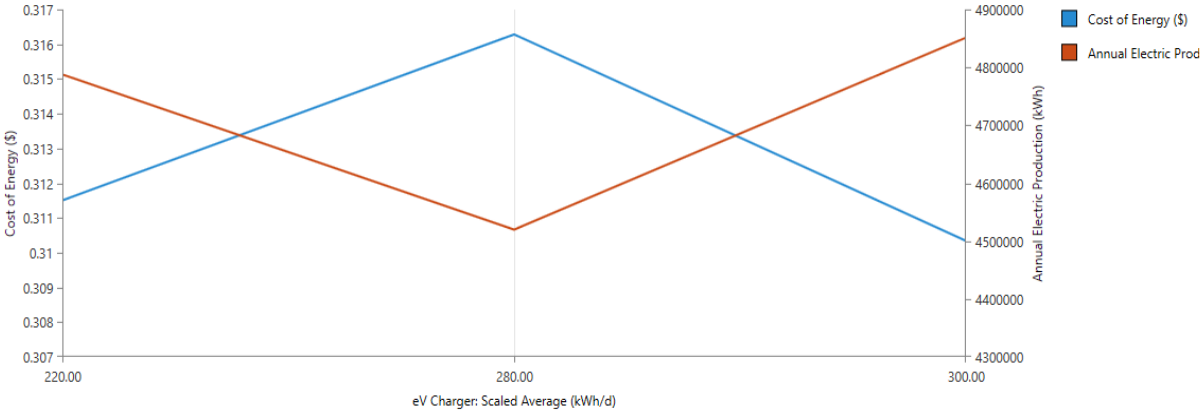

(a)

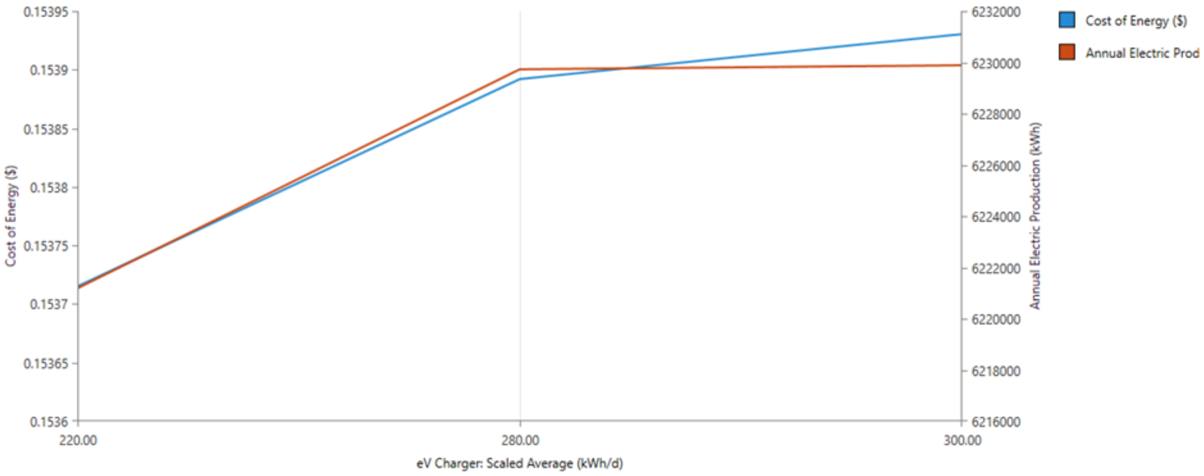

(b)

Figure 14. Average daily electricity consumption impact on the electric charging stations (a) Off-grid and (b) On-Grid.

6.2 Optimization Results

The optimization results of the components used in the systems play a crucial role. A detailed examination of these results allows us to identify components that negatively affect system performance. Figure 15 (a) shows the output power values obtained from the solar panels used in the first off-grid scenario. As expected, the highest efficiency was achieved during midday when the sun's rays reached Earth at the steepest and most intense angles. However, during winter, there is a noticeable drop in the output power. The solar panels operate for 3,857 hours annually, generating a total of 2,328,767 kWh/year of electricity. The cost per unit of electricity produced by the panels is $0.220/kWh.

Quantity	Value	Units
Rated Capacity	2,375	kW
Mean Output	266	kW
Mean Output	6,380	kWh/d
Capacity Factor	11.2	%
Total Production	2,328,767	kWh/yr

Quantity	Value	Units
Minimum Output	0	kW
Maximum Output	1,778	kW
PV Penetration	57.5	%
Hours of Operation	3,857	hrs/yr
Levelized Cost	0.220	$/kWh

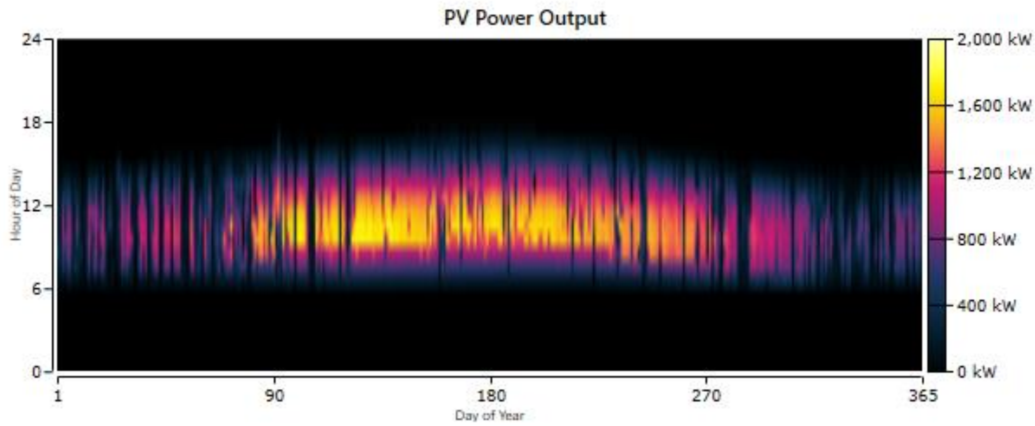

(a)

Quantity	Value	Units
Rated Capacity	1,994	kW
Mean Output	223	kW
Mean Output	5,356	kWh/d
Capacity Factor	11.2	%
Total Production	1,954,893	kWh/yr

Quantity	Value	Units
Minimum Output	0	kW
Maximum Output	1,492	kW
PV Penetration	48.2	%
Hours of Operation	3,857	hrs/yr
Levelized Cost	0.220	$/kWh

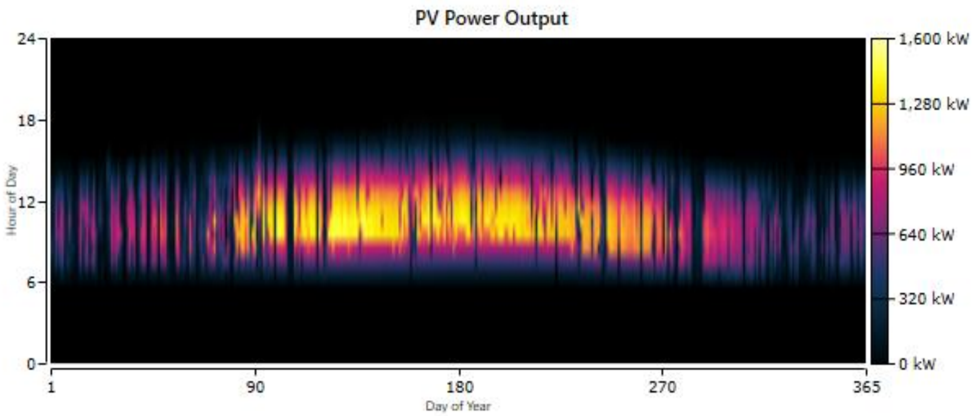

(b)

Figure 15. Solar panel power (a) Off-grid and (b) On-grid.

Figure 15 (b) shows the output power values generated by the solar panels in the second on-grid scenario. The panels operate for a total of 3,857 hours per year, producing 1,954,893 kWh of electricity annually. The cost per kilowatt hour (kWh) of the electricity generated by the panels was calculated as $0.220/kWh.

Quantity	Value	Units
Batteries	7,809	qty.
String Size	1.00	batteries
Strings in Parallel	7,809	strings
Bus Voltage	6.00	V

Quantity	Value	Units
Autonomy	13.2	hr
Storage Wear Cost	0.193	$/kWh
Nominal Capacity	7,809	kWh
Usable Nominal Capacity	6,247	kWh
Lifetime Throughput	23,427,000	kWh
Expected Life	11.7	yr

Quantity	Value	Units
Average Energy Cost	0.0351	$/kWh
Energy In	2,111,347	kWh/yr
Energy Out	1,904,390	kWh/yr
Storage Depletion	4,404	kWh/yr
Losses	211,361	kWh/yr
Annual Throughput	2,007,403	kWh/yr

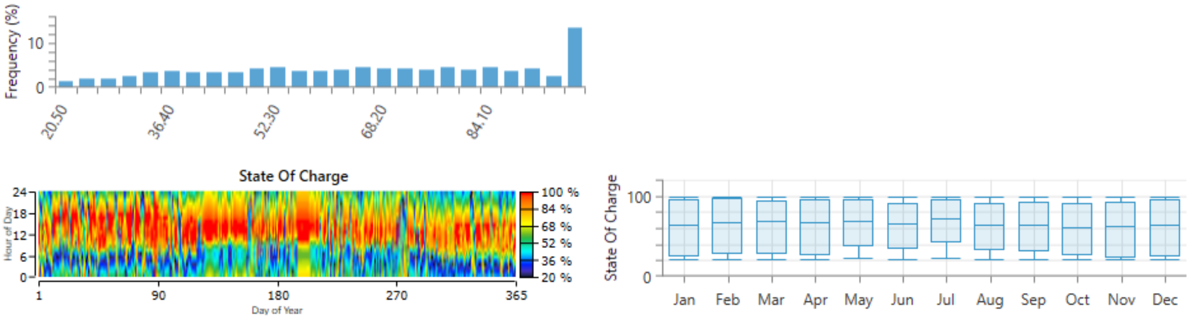

(a)

Quantity	Value	Units
Batteries	21.0	qty.
String Size	1.00	batteries
Strings in Parallel	21.0	strings
Bus Voltage	6.00	V

Quantity	Value	Units
Autonomy	0.0356	hr
Storage Wear Cost	0.193	$/kWh
Nominal Capacity	21.0	kWh
Usable Nominal Capacity	16.8	kWh
Lifetime Throughput	252	kWh
Expected Life	15.0	yr

Quantity	Value	Units
Average Energy Cost	2.54	$/kWh
Energy In	17.7	kWh/yr
Energy Out	15.9	kWh/yr
Storage Depletion	0	kWh/yr
Losses	1.77	kWh/yr
Annual Throughput	16.8	kWh/yr

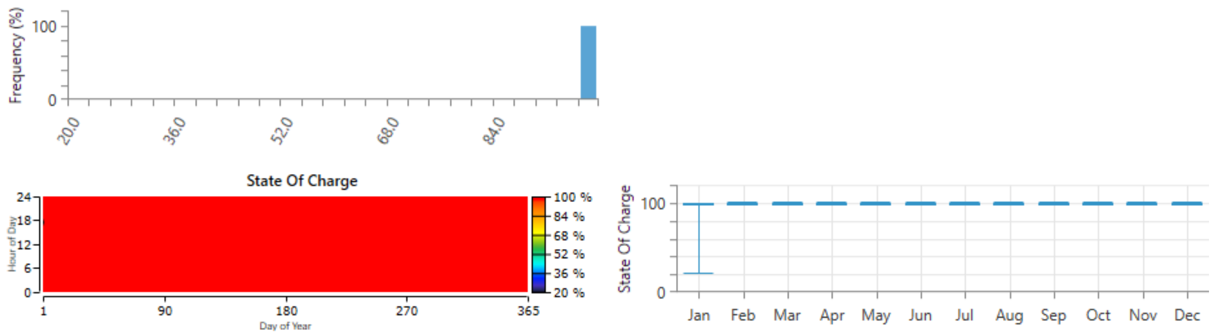

(b)

Figure 16. Battery charge rate (a) Off-grid and (b) On-grid.

In Figure 16 (a), the state of charge (SOC) levels of the batteries used in the first off-grid scenario are presented, reflecting variations across different days and hours throughout the year. During the months when the solar panels operate at peak efficiency, particularly between April and October, the batteries reach full charge (100%) during midday. However, during other hours of the day, and especially in January, February, March, November, and December, the charge levels drop to between 25% and 36%. Nevertheless, the fact that the batteries only reached their minimum state of charge during the least sunny months indicates that the system was equipped with sufficient batteries to meet the demand.

In Figure 16 (b), the state of charge (SOC) levels of the batteries used in the second on-grid scenario are illustrated, showing variations across different days and hours throughout the year. As shown in the figure, the battery charge levels remained consistently at 100% throughout the year. This can be attributed to the fact that the system is connected to the grid, ensuring a continuous supply of electricity that maintains full battery capacity at all times.

Quantity	Value	Units
Hours of Operation	1,657	hrs/yr
Number of Starts	360	starts/yr
Operational Life	9.05	yr
Capacity Factor	16.6	%
Fixed Generation Cost	112	$/hr
Marginal Generation Cost	0.0401	$/kWh

Quantity	Value	Units
Electrical Production	2,476,369	kWh/yr
Mean Electrical Output	1,494	kW
Minimum Electrical Output	540	kW
Maximum Electrical Output	1,700	kW

Quantity	Value	Units
Fuel Consumption	627,233	m^3
Specific Fuel Consumption	0.253	m^3/kWh
Fuel Energy Input	6,193,926	kWh/yr
Mean Electrical Efficiency	40.0	%

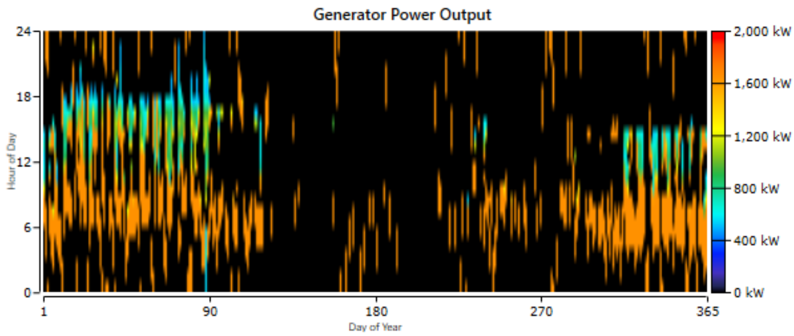

(a)

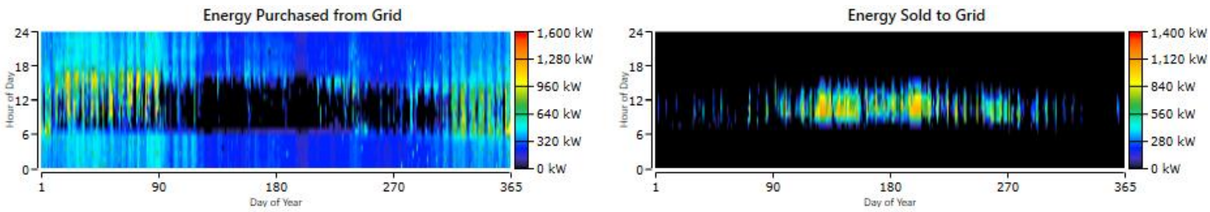

(b)

Figure 17. The amount of electrical energy purchased and sold from the grid (a) Off-Grid, (b) On-Grid.

Figure 17 (a) shows the output power values of the natural gas generator used in the first off-grid scenario, highlighting variations across different days and hours throughout the year. As the figure illustrates, the use of batteries and solar panels in the system significantly reduces the reliance on electricity generated by the natural gas generator. The generator was operated for 1,657 hours over the course of the year, producing 2,476,369 kWh of electricity. The cost per kilowatt hour (kWh) of the electricity generated by the generator was calculated as $0.0401/kWh. Notably, between days 90 and 300 of the year, the generator was scarce. This indicates that sufficient energy is supplied by the solar panels, and during non-sunny hours, energy is drawn from the battery storage.

In Figure 17 (b), the quantities of electricity purchased from and sold to the grid in the second on-grid scenario are illustrated for different periods throughout the year. The system drew 1,580,932 kWh from the grid over the course of the year and sold 3,053,852 kWh back to the grid. These figures indicate that the system's components were able to meet the system's energy demands for the majority of the time, often producing excess electricity. The surplus energy was sold back to the grid, resulting in a financial gain for the system.

Production	kWh/yr	%
SunPower E20-327	1,954,893	41.2
Grid Purchases	2,785,705	58.8
Total	4,740,598	100

Consumption	kWh/yr	%
AC Primary Load	4,052,912	87.3
DC Primary Load	0	0
Deferrable Load	80,182	1.73
Grid Sales	509,755	11.0
Total	4,642,850	100

Quantity	kWh/yr	%
Excess Electricity	0	0
Unmet Electric Load	0	0
Capacity Shortage	0	0

Quantity	Value	Units
Renewable Fraction	40.0	%
Max. Renew. Penetration	105	%

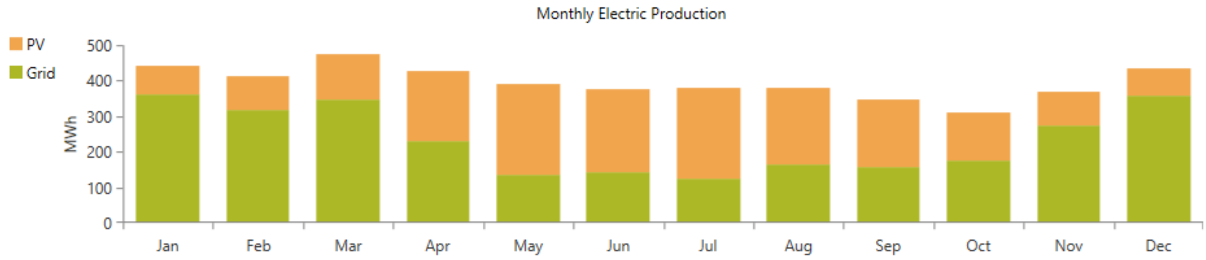

(a)

Production	kWh/yr	%
SunPower E20-327	2,328,767	48.5
Autosize Genset	2,476,369	51.5
Total	4,805,136	100

Consumption	kWh/yr	%
AC Primary Load	4,052,912	98.1
DC Primary Load	0	0
Deferrable Load	80,172	1.94
Total	4,133,084	100

Quantity	kWh/yr	%
Excess Electricity	240,360	5.00
Unmet Electric Load	0	0
Capacity Shortage	0	0

Quantity	Value	Units
Renewable Fraction	40.1	%
Max. Renew. Penetration	1,144	%

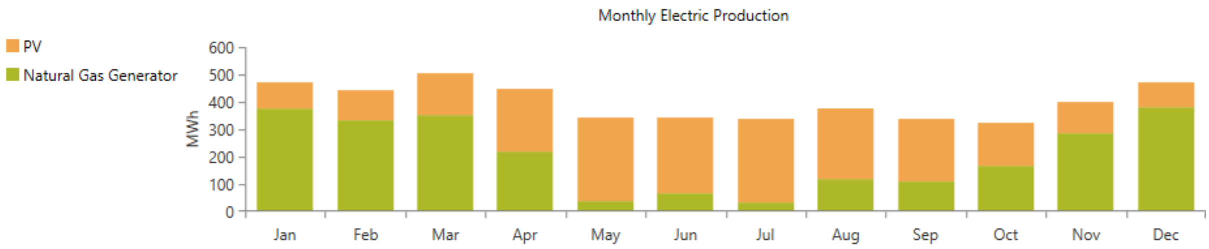

(b)

Figure 18. Distribution of electricity production (a) Off-grid and (b) On-grid.

Figure 18 (a) presents the monthly electricity generation breakdown of the system components in the second on-grid scenario. The data indicate that 41.2% of the system's annual electricity demand is met by solar panels, whereas the remaining 58.8% is covered by electricity purchased from the grid. Over the course of a year, the solar panels generated 1,954,893 kWh, whereas the total electricity drawn from the grid was 2,785,705 kWh. This highlights the reliance on grid electricity to complement renewable energy generation, particularly during periods of low solar output.

Figure 18 (b) illustrates the monthly electricity generation breakdown for the first off-grid scenario. The analysis shows that 48.5% of the system's total annual electricity generation is supplied by solar panels, whereas the natural gas generator contributes 51.5%. The figure also indicates that during the summer months, the solar panels are able to meet nearly the entire system's electricity demand. Annually, the solar panels produced 2,328,767 kWh of electricity, while the natural gas generator generated a total of 2,476,369 kWh. This distribution reflects the seasonal variability in solar energy production, with the generator compensating for the reduced solar output during winter and low-irradiance periods.

6.3 Cost Analysis

A hybrid energy system designed to meet the 2024 electricity consumption requirements of the Yeni Yalova State Hospital, which is located 5.5 km from the Yalova city center, was modeled by incorporating the data defined in the system components section into the simulation. The optimal simulation results for four different on-grid system scenarios are presented in Table 2, and the off-grid simulation results are detailed in Table 2. These tables provide a comprehensive comparison of system performance under both grid-connected and standalone operational conditions, providing insights into the cost-effectiveness and energy efficiency of each scenario.

Table. 1 On grid scenario results.

Scenario	PV (kW)	WT (kW)	Generator (kW)	Battery (kWh)	Converter (kW)	NPC ($)	COE ($)	Fuel
1	3464	----	--	7	2514	18M	0,154	Biogas
2	1994	----	----	24	1451	15,5M	0,173	Natural gas
3	3456	----	--	46	2541	18M	0,154	Diesel
4	3482	4	1700	20	2549	18,4M	0,157	Biodiesel

Table 2. Off grid scenario results.

Scenario	PV (kW)	WT (kW)	Generator (kW)	Battery (kWh)	Converter (kW)	NPC ($)	COE ($)	Fuel
1	2375	----	1700	7809	1946	26.2M	0,327	Biogas
2	6114	----	1700	10173	1527	39,0M	0,488	Natural gas
3	2589	----	1700	7728	1398	39,5M	0,493	Diesel
4	3113	----	1700	10477	1348	42,9M	0,536	Biodiesel

As evidenced by the tables, the selected system components in the analyzed scenarios include the grid connection (on-grid), Solar Panels, Wind Turbines, Generators, and Batteries. Variations in system design were applied to the generator selection, component configurations, renewable energy penetration levels, wind turbine height, unit natural gas prices, electric vehicle charging loads, power capacity, and annual consumption to identify the most optimal system configuration.

A detailed analysis of the scenario results indicates that the second on-grid scenario, which incorporates a hybrid energy system with PVs and batteries, is the most cost-effective configuration, with a net present cost of $15.5 million and a unit energy cost of $0.173/kWh. In contrast, for the off-grid configuration, the first scenario—comprising Solar Panels, a Natural Gas Generator, and Batteries—was found to be the optimal solution from a cost perspective, with a net present cost of $26.2 million and a unit energy cost of $0.327/kWh.

This analysis demonstrates that the integration of renewable energy sources, particularly in grid-connected systems, significantly reduces both the net present and unit energy costs. However, in off-grid systems, while reliance on renewable energy is still beneficial, the inclusion of a backup generator is critical for ensuring system reliability, particularly in periods of low solar or wind resource availability.

6.4 Lowest-Cost Scenario

In energy system design, cost efficiency plays a critical role in achieving both economic and environmental sustainability. On-grid energy systems, which operate by interfacing with the electrical grid, offer high efficiency and low operational costs. In this context, On-Grid Scenario 2 is the lowest-cost scenario due to its advantageous features and cost-effectiveness.

One of the key benefits of Scenario 2 is its notably low unit energy cost, calculated at $0.173/kWh. This cost efficiency is due to the combination of solar panels (1,994 kW) and inverters (1,451 kW), enabling efficient energy conversion and maximizing production. The substantial solar panel capacity supports a significant level of energy generation, while the high inverter capacity ensures efficient conversion of this energy to alternating current (AC). Furthermore, a grid connection provides the ability to draw electricity from the grid when required, which mitigates the limitations of battery storage and enhances the overall reliability of the system.

The total installation and maintenance cost of the proposed system was estimated to be $15.5 million. Despite the relatively high upfront capital expenditure, the low unit energy cost and substantial energy production capacity provide significant long-term savings, ultimately improving the system's economic viability. These characteristic position On-Grid Scenario 2 as the most cost-effective energy solution among the scenarios analyzed.

6.5 Environmental Assessment

In addition to the cost outcomes, the emission values of the scenarios play a critical role in reducing environmental impacts. Table 3 presents the emission values for both the on-grid and off-grid scenarios.

Table 3. Emission values.

Product	**On-Grid (kg/year)**	**Off-Grid (kg/year)**
Carbon Dioxide (CO_2)	1,760,565	1,199,940
Carbon Monoxide (CO)	0	10,349
Unburned Hydrocarbons	0	452
Particulate Matter	0	62.7
Sulfur Dioxide (SO_2)	7,633	0
Nitrogen Oxides (NO_x)	3,733	9,722

The HOMER simulation indicates that 40% of the electricity generated in Scenario 2 will be sourced from renewable energy. Similarly, for off-grid Scenario 1, 40% of the electricity is also derived from renewable energy sources.

7. CONCLUSION

In this study, hybrid energy systems—both grid-connected and off-grid—were designed using HOMER software to meet the 2024 monthly electricity demand of the new Yalova State Hospital, which is located 5.5 km from the Yalova city center. Various scenarios were developed and analyzed to determine the most optimal system configuration. The main components of these systems include solar panels, wind turbines, natural gas generators, inverters, and batteries. Differences among the scenarios arise from variations in the system components and sensitivity analyses, including the addition or removal of generators and grid connections. Through these analyses, the most suitable system to meet the hospital's energy demand was identified.

The results indicate that the hybrid energy system comprising solar panels, the grid, and batteries, with a net present cost of $15.5 million and a unit energy cost of $0.173/kWh, was the most cost-efficient solution. This system also achieves a 40% share of renewable energy, further enhancing its cost-effectiveness and environmental sustainability. However, if the objective is to operate independently from the grid and focus more on environmental considerations, the first off-grid scenario presents a reasonable alternative. This system, which features solar panels, a natural gas generator, and batteries, has a net present cost of $26.2 million and a unit energy cost of $0.327/kWh.

Given the current balance between cost and renewability, on-grid Scenario 2 emerges as a more practical option in today's energy landscape. This conclusion is based not only on lower costs but also on the system's integration of a substantial percentage of renewable energy.

Future Recommendations

1. **Feasibility Studies on Renewable Potential:** Before implementing renewable energy systems, conducting detailed feasibility studies that assess the solar and wind energy potential of selected sites is essential. Accurate meteorological data are crucial for optimizing the system performance and ensuring that the design aligns with local energy resources.

2. **Demand Assessment:** A thorough assessment of the facility's energy load requirements is vital for system sizing and efficiency. Fluctuations in electricity demand should be factored into the system design, especially when considering hybrid systems that combine renewable and conventional energy sources.

3. **Adaptability to Future Energy Needs:** As energy consumption patterns evolve, hybrid systems should be designed with flexibility in mind. Systems should be adaptable to incorporate future technologies, such as advanced energy storage solutions, demand-side management, and vehicle-to-grid (V2G) applications, as electric vehicle use becomes more widespread.

4. **Environmental considerations: Although** cost remains a critical factor, future energy projects should prioritize sustainability. Off-grid systems may become more attractive as the cost of renewable energy technologies continues to decrease and environmental regulations tighten. The shift toward fully renewable energy systems, even in off-grid configurations, should be a key long-term goal.

5. **Policy and Incentive Programs:** Governments and regulatory bodies should support the deployment of hybrid renewable energy systems through policy measures, incentives, and subsidies. These initiatives can make on-grid and off-grid systems more financially viable and accelerate the transition toward greener energy solutions.

6. **Technology Integration and Optimization:** Continued advancements in energy storage, inverter technologies, and grid management systems are essential for maximizing the efficiency of hybrid systems. Future projects should leverage these technological developments to improve the resilience and reliability of energy systems, particularly in off-grid applications.

In conclusion, while grid-connected systems provide a balance between cost efficiency and renewability, off-grid systems offer enhanced energy independence. Both configurations have significant roles to play in the future energy landscape, and careful planning, combined with ongoing technological advancements, is critical to achieving sustainable and resilient energy systems.

AUTHORS' CONTRIBUTIONS

All authors contributed equally to the study.

STATEMENT OF INTEREST CONFLICTS

The authors declare no conflict of interest.

STATEMENT OF RESEARCH AND PUBLICATION ETHICS

The author declares that this study complies with Research and Publication Ethics.

REFERENCES

Al-Sahlawi A.A.K, Ayob S.M., Tan C.W., et al (2024). Optimal Design of Grid-Connected Hybrid Renewable Energy System Considering Electric Vehicle Station Using Improved Multi-Objective Optimization: Techno-Economic Perspectives. Sustain 16:. https://doi.org/10.3390/su16062491

Belkhier Y., Oubelaid A., Shaw R.N. (2024). Hybrid power management and control of fuel cells-battery energy storage system in hybrid electric vehicle under three different modes. Energy Storage 6:1–22. https://doi.org/10.1002/est2.511

Chowdhury, S., Kumar, Y., Shrivastava, S., Patel, S. K., & Sangwai, J. S. (2023). A Review on the Recent Scientific and Commercial Progress on the Direct Air Capture Technology to Manage Atmospheric CO2 Concentrations and Future Perspectives. Energy & Fuels, 37(15), 10733–10757. doi: 10.1021/acs.energyfuels.2c03971

Diaf, S., Notton, G., Belhamel, M., Haddadi, M., & Louche, A. (2008). Design and techno-economical optimization for hybrid PV/wind system under various meteorological conditions. Applied Energy, 85(10), 968–987. doi: 10.1016/j.apenergy.2008.02.012

Falope T., Lao L., Hanak D., Huo D. (2024). Hybrid energy system integration and management for solar energy: A review. Energy Convers Manag X 21:100527. https://doi.org/10.1016/j.ecmx.2024.100527

Guven A.F. (2024). Integrating electric vehicles into hybrid microgrids: A stochastic approach to future-ready renewable energy solutions and management. Energy 303:131968. https://doi.org/10.1016/j.energy.2024.131968

Güven A.F. &Yücel E. (2024). Sustainable energy integration and optimization in microgrids: enhancing efficiency with electric vehicle charging solutions. Electr Eng. https://doi.org/10.1007/s00202-024-02619-x

Güven A.F. & Yörükeren N. (2024). A comparative study on hybrid GA-PSO performance for stand-alone hybrid energy systems optimization. 42:1410–1438. https://doi.org/10.14744/sigma.2024.00

Güven, A. F. & Mete M. (2021). Balıkesir İli Erdek İlçesi İçin Bağımsız Hibrit Enerji Sisteminin Fizibilite Çalışması Ve Ekonomik Analizi. KONJES, c. 9, sy. 4, ss. 1063–1076, 2021, doi: 10.36306/konjes.978002.

Güven, A. F. (2017). Bahçelievler Belediye Başkanlık Binasının Enerji İhtiyacının Güneş ve Rüzgar Sistemi ile Karşılanması, Optimizasyonu ve Maliyet Analizi. Sinop Üniversitesi Fen Bilimleri Dergisi, 2(1), 24–36. Retrieved from http://dergipark.gov.tr/sinopfbd/issue/28364/255023.

Güven, A. F., & Hatipoğlu, C. (2022). Şebekeden Bağımsız Güneş/Rüzgâr/Biyogaz/Yakıt Hücresi/Batarya Tabanlı Hibrit Enerji Sisteminin Tekno-Ekonomik Analizi: Muğla Zaferler Köyü Vaka Çalışması. EMO Bilimsel Dergi, 12(1), 53-65.

Güven, A. F., & Mengi, O. Ö. (2023). Assessing metaheuristic algorithms in determining dimensions of hybrid energy systems for isolated rural environments: Exploring renewable energy systems with hydrogen storage features. Journal of Cleaner Production, 428(September). doi: 10.1016/j.jclepro.2023.139339

Güven, A. F., & Poyraz, E. (2021). Feasibility Study and Techno-Economic Analysis of Stand-Alone Hybrid Energy System for Muğla Province Köyceğiz. Karadeniz Fen Bilimleri Dergisi, 11(1), 70–85. doi: 10.31466/kfbd.880437.

Güven, A. F., & Yörükeren, N. (2022). Bir Hibrit Enerji Sisteminin Parçacık Sürüsü Optimizasyon Algoritması- Genetik Algoritma ve Gri Kurt Optimizasyon Algoritma Tekniği ile Enerji Yönetimi ve Optimizasyonu: Yalova Üniversitesi için bir vaka çalışması. Karadeniz Fen Bilimleri Dergisi, 12(2), 853–879. doi: 10.31466/kfbd.1169643

Güven, A. F., & Yücel, E. (2023). Application of HOMER in assessing and controlling renewable energy-based hybrid EV charging stations across major Turkish cities. International Journal of Energy Studies, 8(4), 747–780. doi: 10.58559/ijes.1324236.

Güven, A. F., Türkmen, Ş., Aşıklı, E., & Örnek, G. (2023). Investigating the Effects of Different Types of Battery Impacts in Energy Storage Systems on Standalone Hybrid Renewable Energy Systems. Karadeniz Fen Bilimleri Dergisi, 13(3), 943–964. doi: 10.31466/kfbd.1275823.

Hasanien H.M., Alsaleh I., Tostado-Véliz M., et al (2024). Hybrid particle swarm and sea horse optimization algorithm-based optimal reactive power dispatch of power systems comprising electric vehicles. Energy 286:. https://doi.org/10.1016/j.energy.2023.129583

Jui J.J., Ahmad M.A., Molla M.M.I., Rashid M.I.M. (2024). Optimal energy management strategies for hybrid electric vehicles: A recent survey of machine learning approaches. J Eng Res 12:454–467. https://doi.org/10.1016/j.jer.2024.01.016